ANNALS OF MEDICINE
2023, VOL. 55, NO. 2, 2237690
https://doi.org/10.1080/07853890.2023.2237690

RESEARCH ARTICLE

OPEN ACCESS Check for updates

Paracrine effects of mir-210-3p on angiogenesis in hypoxia-treated c-kit-positive cardiac cells

Louyi Shen[a,b,c], Guan Fan[a,b,c], Guoliang Yang[a,b,c], Zhijie Yang[d] and Chun Gui[a,b,c]

[a]Department of Cardiology, The First Affiliated Hospital of Guangxi Medical University, Nanning, China; [b]Guangxi Key Laboratory Base of Precision Medicine in Cardiocerebrovascular Diseases Control and Prevention, Nanning, China; [c]Guangxi Clinical Research Center for Cardiocerebrovascular Diseases, Nanning, China; [d]Department of Cardiology, Liuzhou People's Hospital, Liuzhou, China

ABSTRACT

Objective: Treatment with c-kit-positive cardiac cells (CPCs) has been shown to improve the prognosis of ischemic heart disease. MicroRNAs (miRNAs) confer protection by enhancing the cardiac repair process, but their specific functional mechanisms remain unclear. This study aimed to screen for differentially expressed miRNAs in CPCs under hypoxia and explore their effects on the function of CPCs.

Methods: We harvested CPCs from C57 adult mice and later performed a high-throughput miRNA sequencing for differential expression profiling analysis. Subsequently, we intervened with the differentially expressed gene miR-210-3p in CPCs and detected changes in the secretion of angiogenesis-related factors through a protein-chip analysis. Finally, we applied CPC supernatants of different groups as conditioned medium to treat mouse cardiac microvascular endothelial cells (CMECs) and further investigated the functional effects of miR-210-3p on c-kit+CPCs under ischemia and hypoxia conditions.

Results: The miR-210-3p was highly increased in hypoxia-treated CPCs. Protein-chip detection revealed that CPCs expressed cytokines such as FGF basic, angiogenin, and vascular endothelial growth factor (VEGF) and that hypoxia enhanced their release. Silencing miR-210-3p resulted in a reduction in the release of these angiogenesis-related factors. In addition, the conditioned medium of hypoxia-treated CPCs promoted the proliferation, migration, and tube-forming capabilities of CMECs. In contrast, the conditioned media of CPCs with silenced miR-210-3p after hypoxia decreased the proliferation, migration, and tube-forming ability of CMEC.

Conclusions: The CPCs exert proangiogenic effects via paracrine pathways mediated by miR-210-3p. Upregulation of miR-210-3p in hypoxia-treated CPCs may enhance their paracrine function by regulating the secretion of angiogenic factors, thereby promoting angiogenesis in ischemic heart disease.

ARTICLE HISTORY
Received 11 May 2023
Revised 1 July 2023
Accepted 12 July 2023

KEYWORDS
c-kit-positive cardiac cells; hypoxia; miR-210-3p; paracrine functions; ischemic cardiomyopathy

1. Introduction

Ischemic cardiomyopathy (ICM) is primarily caused by ventricular dysfunctions due to reduced contractile functions and/or changes in diastolic functions. The global incidences of ICM have increased and the mortality rate remains high. Without timely and effective interventions to control this condition, the treatment-associated challenges will increase [1]. Stem cell transplantation for ICM treatment has become a focus of research in cardiac regeneration medicine [2].

The c-kit-positive cardiac cells (CPCs) have potential applications in regenerative medicine for heart disease. The CPCs were first identified in 2003 when Beltrami et al. [3] discovered an assortment of cells in cardiac tissues expressing the c-kit receptor. This receptor is a marker of stem cells, and its presence suggests that these cells have the ability to regenerate damaged heart tissues. Li et al. [4] injected CPCs into infarcted heart areas myocardial infarction-mice models. The CPCs developed into multiple cardiac cell lineages, resulting in increased myocardial mass and reduced scar sizes, promoting cardiac cell rejuvenation and restoring cardiac functions. This suggests that CPCs have the potential to treat heart disease. Subsequent investigations revealed that CPCs have a lower retention rate and are rapidly depleted from the recipient myocardium. They can secrete a diverse array of cytokines, which improve the viability and regenerative

CONTACT Chun Gui gui_chun@163.com No. 6 Shuangyong Road, Qingxiu District, Nanning, Guangxi Zhuang Autonomous Region, China
© 2023 The Author(s). Published by Informa UK Limited, trading as Taylor & Francis Group
This is an Open Access article distributed under the terms of the Creative Commons Attribution-NonCommercial License (http://creativecommons.org/licenses/by-nc/4.0/), which permits unrestricted non-commercial use, distribution, and reproduction in any medium, provided the original work is properly cited. The terms on which this article has been published allow the posting of the Accepted Manuscript in a repository by the author(s) or with their consent.

capacity of infarcted myocardial cells, leading to improvements in cardiac function. The paracrine effect of CPCs is the main mechanism for improving ventricular functions [5]. These findings imply that CPCs have the potential for cardiac regeneration and repair, and more research should be performed to elucidate on the properties and functions of CPCs and to inform on the development of effective cell-based therapies for cardiac regeneration and repair.

The microRNAs (miRNAs) are tiny noncoding RNA molecules that serve crucial roles in gene control after transcription. They play various roles in biological reactions, including cell proliferation, differentiation and apoptosis. Moreover, they play regulatory roles in occurrence and progression of cardiovascular illnesses, angiogenesis [6], cardiomyocyte apoptosis [7], proliferation and injury of endothelial cells [8], myocardial hypertrophy and fibrosis [9,10], atherosclerosis [11], arrhythmia [12], and other physiological and pathological processes. To enhance angiogenesis, miR-210 suppresses the expressions of antiangiogenic factors [13]. The miRNAs can regulate the proliferation [14], differentiation [15], angiogenesis [16,17], apoptosis, necrosis [18] and paracrine effects [19,20] of cardiac cells.

To simulate the possible *in vivo* environment and clinical conditions of ICM, we subjected CPCs to hypoxic treatment. Then, sequencing was performed to identify the significantly differentially expressed miRNAs in hypoxic CPCs and to determine their potential roles. Our findings elucidate on the potential roles of CPCs in development, progression, adverse prognosis and treatment of ICM.

2. Materials and methods

2.1. Animals

Healthy adult male C57BL/6 mice aged 4–6 weeks were acquired from the Guangxi Medical University's Experimental Animal Center. The license number for animal production is scxk GUI 2020-0003. All animals were fed in strict accordance with SPF level animal feeding rules. All protocols were approved by Guangxi Medical University's Animal Ethics Committee and were performed in accordance with the National Institutes of Health Guidelines for the Care and Use of Laboratory Animals.

2.2. Isolation of CPCs

Hearts of healthy adult male C57BL/6 mice aged 4–6 weeks were harvested, sliced into small pieces, digested in a mixture of 0.25% trypsin and 0.1% type II collagenase and preheated thrice at 37 °C. The resulting cells were filtered through a 70-μm mesh, and cultured in a complete explant medium (CEM) at 37 °C and 5% CO_2. DMEM/F-12 mixed with 10% foetal bovine serum (Gibco, Carlsbad, CA), 2 mmol/L L-glutamine (Solarbio, Beijing, China), 100 units/mL penicillin G (Gibco, Carlsbad, CA) and 100 mg/mL streptomycin (Gibco, Carlsbad, CA) comprised CEM. After five days of culture, a covering of small, spherical, phase-bright cells was formed in the cell culture flask. Cells were collected and subjected to enzymolysis with 0.25% trypsin, followed by magnet-activated c-kit cell separation with anti-c-kit-coupled magnet beads (Miltenyi Biotec, Bergisch Gladbach, Germany), as directed by the manufacturer.

2.3. Culture of CPCs

Sorted cells were cultured in cardiosphere-growth medium (CGM) at 37 °C and 5% CO_2. The CGM was made up of CEM supplemented with 2% B27 (Thermo Fisher, Waltham, MA), 20 ng/mL basic fibroblast growth factor (bFGF) (Sino Biological, Beijing, China), 10 ng/mL epidermal growth factor (EGF) (Sino Biological, Beijing, China) and 10 ng/mL leukaemia inhibitory factor (LIF) (Miltenyi Biotec, Bergisch Gladbach, Germany).

2.4. Immunofluorescence staining

To fix the CPCs, a 4% paraformaldehyde solution was used when the percentage of cells attached to the slide was approximately 60%. The cells were blocked with 5% goat serum and treated overnight at 4 °C with the c-kit primary antibody (eBioscience, San Diego, CA). Subsequently, cells were incubated for 1 h at room temperature with secondary antibodies away from light. Finally, the slides were then stained with DAPI.

2.5. Flow cytometry

When the percentage of CPCs that had adhered to the slide was 90%, cells were prepared into a single-cell solution. Then, they were stained with either an anti-c-kit (eBioscience, San Diego, CA) or IgG isotype control (eBioscience, San Diego, CA) PE-conjugated antibody. The positive rate of c-kit or isotype control in the total cell population was detected by FACS Calibur flow cytometry.

2.6. Hypoxia preconditioning

The CPCs were washed thrice using PBS, cultivated in CGM without foetal bovine serum and randomized into two groups: control and hypoxia. Control group

cells were cultivated in an ordinary cell incubator for 12 h, while hypoxia group cells were placed in a hypoxia incubator chamber filled with a mixture of 5% CO_2 and 95% N_2. Cells were incubated at 37 °C for 12 h after the chamber was tightly closed.

2.7. RNA isolation, small RNA library construction and sequencing

Total RNA was extracted from control and hypoxia groups using the RNAiso Plus reagent (TaKaRa, Maebashi, Japan), as instructed by the manufacturer. RNA purity was assessed using Nano Drop 2000 (Thermo Fisher, Waltham, MA), while its concentration was determined using a Thermo Fisher Invitrogen Qubit 3.0 Spectrophotometer. RNA integrity was determined using an Agilent 2100 Bioanalyzer (Agilent Technologies, Santa Clara, CA). The quality criteria for RNA samples were: RNA integrity number ≥8.0, 1.8 < OD260/280 < 2.0 and minimum RNA sample concentration of ≥200 ng/μL.

Qualified RNAs were selected to construct a high-quality small RNA sequencing library downstream, which was then sent to Genesky Bio-Tech Co., Ltd. (Shanghai, China) for small RNA library construction and next-generation sequencing. Recovered small RNAs were purified from polyacrylamide gels and used to construct a library. Different samples were directly used for RNA sequencing and differential expression analysis using a HiSeq 2500 Sequencing System (Illumina, San Diego, CA). The Deseq2 software was used to identify genes that were differently expressed between the groups. Standard selection criteria were established to identify differentially expressed miRNAs between the control and hypoxia groups, with a $|\log2(\text{fold-change})| > 1$ and $p < .05$. ClusterProfiler was used to assess gene enrichment and functional annotation based on Gene Ontology (GO) and Kyoto Encyclopedia of Genes and Genomes (KEGG). Adjusted $p < .05$ was considered significantly enriched in the GO and KEGG pathway enrichment analyses. The GEO Series accession number GSE229934 was assigned to all microarray data deposited in the NCBI Gene Expression Omnibus.

2.8. Quantitative real-time PCR (qRT-PCR) assays

The Mir-X miRNA First-Strand Synthesis Kit (TaKaRa, Maebashi, Japan) was used for converting total RNA from each sample into cDNA to enable quantification of miRNAs by real-time PCR. qRT-PCR was performed on an Applied Biosystems 7500 Real-Time PCR System (Thermo Fisher, Waltham, MA) using the Mir-X miRNA qRT-PCR SYBR Kit (TaKaRa, Maebashi, Japan), as instructed by the manufacturer. Primers for target genes were designed using the Mir-X miRNA qRT-PCR SYBR Kit, according to the manufacturer's instructions. Each miRNA was tested in three separate biological replicates from distinct groups in triplicate. The comparative quantity $2^{-\Delta\Delta CT}$ approach was used to determine the relative fold changes in miRNA expressions [21]. The following primer sets were used in this study: U6-Forward: 5′-GGAACGATACAGAGAAGATTAGC-3′, U6-reverse: 5′-TGGAACGCTTCACGAATTTGCG-3′, mmu-miR-210-3p: 5′-ACGTGTGACAGCGGCTGAA-3′, mmu-miR-503-5p: 5′-AGCGGGAACAGTACTGCAGAA-3′, mmu-miR-133b-3p: 5′-TGGTCCCCTTCAACCAGCTA-3′, mmu-miR-877-3p: 5′-CCTCTTCTCCCTCCTCCCAA-3′, mmu-miR-3473b: 5′-TCG TGGAGAGATGGCTCAGAA-3′, mmu-miR-3102-5p.2-5p: 5′-TG CAGGCAGGAGAGCCAA-3′.

2.9. Transfection of CPCs

The CPCs were transfected with a lentiviral vector containing an inhibitor of miRNA-210-3p. Lentiviruses containing the miRNA-210-3p inhibitor or negative control (NC) were constructed by Genechem Co., Ltd. (Shanghai, China). The lentiviral vector (GV280) had the following element sequence: hU6-MCS-Ubiquitin-EGFP-IRES-puromycin, the reverse complementary sequence was TCAGCCGCTGTCACACGCACAG, and the control insertion sequence was TTCTCCGAACGTGTCACGT. GV280 expresses enhanced green fluorescent protein, which facilitates gene delivery. To transfect CPCs, recombinant miRNA-210-3p inhibitor or miRNA-210-3p NC lentiviral vectors were added to the cells, incubated for 12 h, and the medium replaced with a fresh medium. Fluorescent protein signals were detected by fluorescence microscopy. The obtained groups of transfected CPCs were miR-210-3p inhibitor group and miRNA-210-3p NC group. Both cell groups were treated with anoxia. Total RNA was extracted from the control group (control), hypoxia group (hypoxia), hypoxia + miRNA-210-3p inhibitor group (hypoxia + inhibitor) and hypoxia + miRNA-210-3p NC group (hypoxia + NC) to measure gene transfection efficiency through PCR.

2.10. Conditioned media preparation

Supernatants from each group of cells were centrifuged to remove cell debris and filtered using a 0.22 μm filter to obtain control conditioned medium (CM-C), hypoxia CPCs conditioned medium (CM-H), hypoxia + miR-210-3p inhibitor CPCs conditioned

medium (CM-miR) and hypoxia + miRNA-210-3p NC transfected CPCs conditioned medium (CM-NC). The conditioned media (CM) were stored at 4 °C or −80 °C for further experiments.

2.11. Proteome profiler mouse angiogenesis array

Protein lysates were prepared for the four cell groups, and protein concentrations in each sample determined using a BCA Protein Assay Kit (Beyotime, Nantong, China). The CM and cell protein lysates were analysed with 200 µg of protein from each group with the proteome profiler mouse angiogenesis array ARY015 (R&D Systems, Minneapolis, MN). A Kit with Quick Spots was used to quantify the data. After subtracting the background from each duplicate pair, the relative fold-change was calculated by plotting the average of each group compared to the vehicle control.

2.12. Proliferation assay

Mouse cardiac microvascular endothelial cells (CMECs; cat. no. CP-M129) were acquired from Procell Life Science & Technology Co., Ltd (Wuhan, China). A total of 3000 CMECs were inoculated into each well of a 96-well plate (six replicates per group) and cultured in four different CM mixed at a ratio of 1:1 with the complete CMEC medium. The group without cells was the blank control. On days 0, 1, 2, 3 and 4, 10 µL CCK-8 solution and 100 µL fresh CMECs complete medium were supplemented into each well, and the plate was incubated for 1 h at 37 °C. The absorbance of each well at 450 nm was measured using a microplate reader (Thermo Fisher, Waltham, MA). Cell proliferation was expressed as the difference between absorbance of the test and blank control wells.

2.13. Wound healing assay

Culture inserts (Ibidi, Gräfelfing, Germany) were placed in 24-well plates, and CMECs were cultured in two separate chambers. When cells in both chambers reached 90% confluence, the inserts were removed, four different CM were added to replace the complete medium, and incubated for 72 h. Cell imaging was performed and the ImageJ software (Bethesda, MD) was used to measure the area covered by the cells within the defined gap.

2.14. Transwell migration assay

Migration assays were performed using the Transwell chambers (Corning, Corning, NY). A total of 4000 CMECs were added to the upper chamber of four different CM, while the lower chamber was filled with complete CMEM media. Assays were performed in triplicate. The non-migrated cells that adhered to the upper surface of the filter membrane were removed with cotton swabs after 24 h of culture. Low surface migration cells were stained with 0.1% crystal violet after being fixed with 4% paraformaldehyde. Inverted light microscope was performed to count the number of migratory cells.

2.15. Tube formation assay

After thawing at 4 °C, Matrigel (BD Biosciences, Franklin Lakes, NJ) was placed in a 96-well plate and incubated at 37 °C for 30 min to solidify. Then, 3000 CMECs/well (three replicates for each group) suspended in four different CM were added to 96-well plates. After 3 h of incubation at 37 °C, tube formation was monitored by inverted microscope. The ImageJ software (Bethesda, MD) was used to calculate the total number of branch points and tube lengths.

2.16. Statistical analysis

The GraphPad Prism 6.0 software (La Jolla, CA) was used for statistical analyses. Date are presented as means ± standard deviation. Comparisons of means among groups were performed by one-way analysis of variance. $p < .05$ was the threshold for statistical significance.

3. Results

3.1. Isolation of CPCs

Cells were obtained from hearts of healthy adult male SPF grade C57BL/6 mice. After enzymatic digestion of the myocardial tissue blocks, mixed cells containing a large number of fibroblasts, endothelial cells and other miscellaneous cells were obtained (Figure 1(A)). The CPCs were separated by positively sorting the c-kit magnet beads and culturing them in CGM. One day after magnet-activated cell sorting, images of CPCs were obtained using an inverted phase-contrast microscope (Figure 1(B)). Cells were stained with an anti-c-kit (red) antibody and counterstained with DAPI (blue), which allowed assessment of expressions of specific c-kit antigens in cells by inverted fluorescent microscopy (Figure 1(C)). Flow cytometry was performed to identify the surface antigenicity of mixed cells before sorting and third generation CPCs after sorting. After analysis of the results using FlowJo software, we

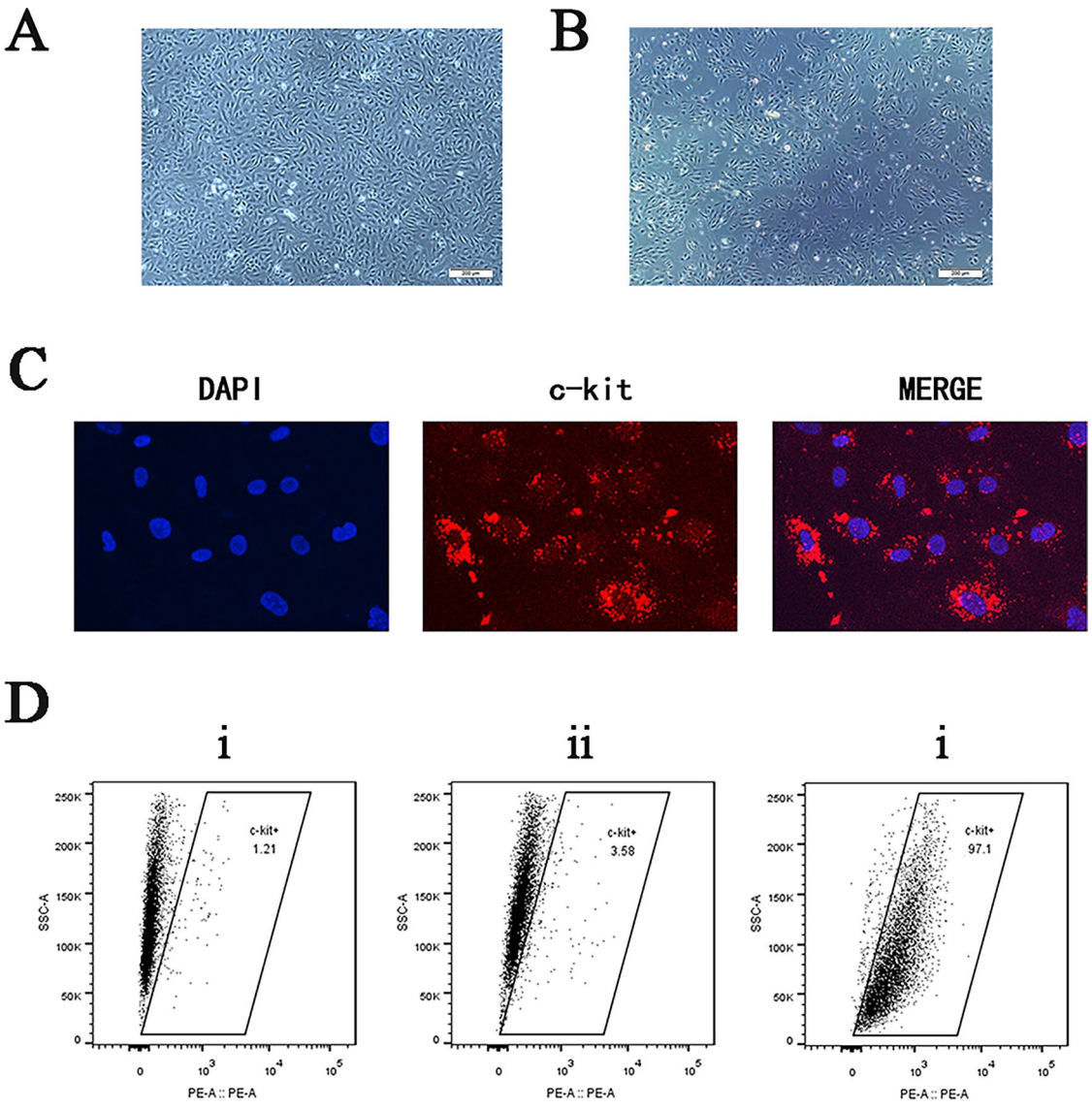

Figure 1. Characterization of cultured CPCs. (A) Prior to sorting, the mixed cell population contained a significant number of fibroblasts and endothelial cells (×40 magnification, scale bar: 200 µm). (B) The sorted CPCs grew well and had spindle-shaped morphologies with relatively uniform cell shapes (×40 magnification, scale bar: 200 µm). (C) Immunofluorescence photographs showing the presence of CD117 (c-kit) in enriched CPCs (×400 magnification). (D) Flow cytometry analysis of the expression of the cell surface marker c-kit in CPCs. (i) The percentage of CD117-positive cells in the unsorted cells was 1.21%. (ii) The percentage of cells positive for the IgG isotype control was 3.58%. (iii) The percentage of CD117-positive cells in the sorted cells was 97.1%.

concluded that the number of CPCs in the mixed cells before sorting was approximately 1.21%, and purity of CPCs in the sorted cells increased to 97.1% (Figure 1(D)). Our analysis showed that the purity of CPCs was significantly improved after magnet bead sorting, and that surface markers of c-kit were stably expressed in cells.

3.2. miRNA-seq of the effects of hypoxia on CPCs

To investigate the molecular mechanisms involved in the effects of hypoxia on paracrine activities of CPCs, miRNA expressions were compared between small RNA libraries of non-hypoxic and hypoxic cell cultures that were maintained for 12 h (Figure 2(A)). To identify differentially expressed miRNAs between the control and hypoxia groups, standard selection criteria were created, which were $|\log2(\text{fold-change})| > 1$, with $p < .05$. Expressions of 23 mature miRNAs in CPCs were significantly altered (14 upregulated and nine downregulated) after exposure to hypoxia for 12 h (Figure 2(B,C)).

We randomly selected six differentially expressed miRNAs (upregulated miRNAs: mmu-miR-210-3p, mmu-miR-503-5p, mmu-miR-133b-3p; downregulated

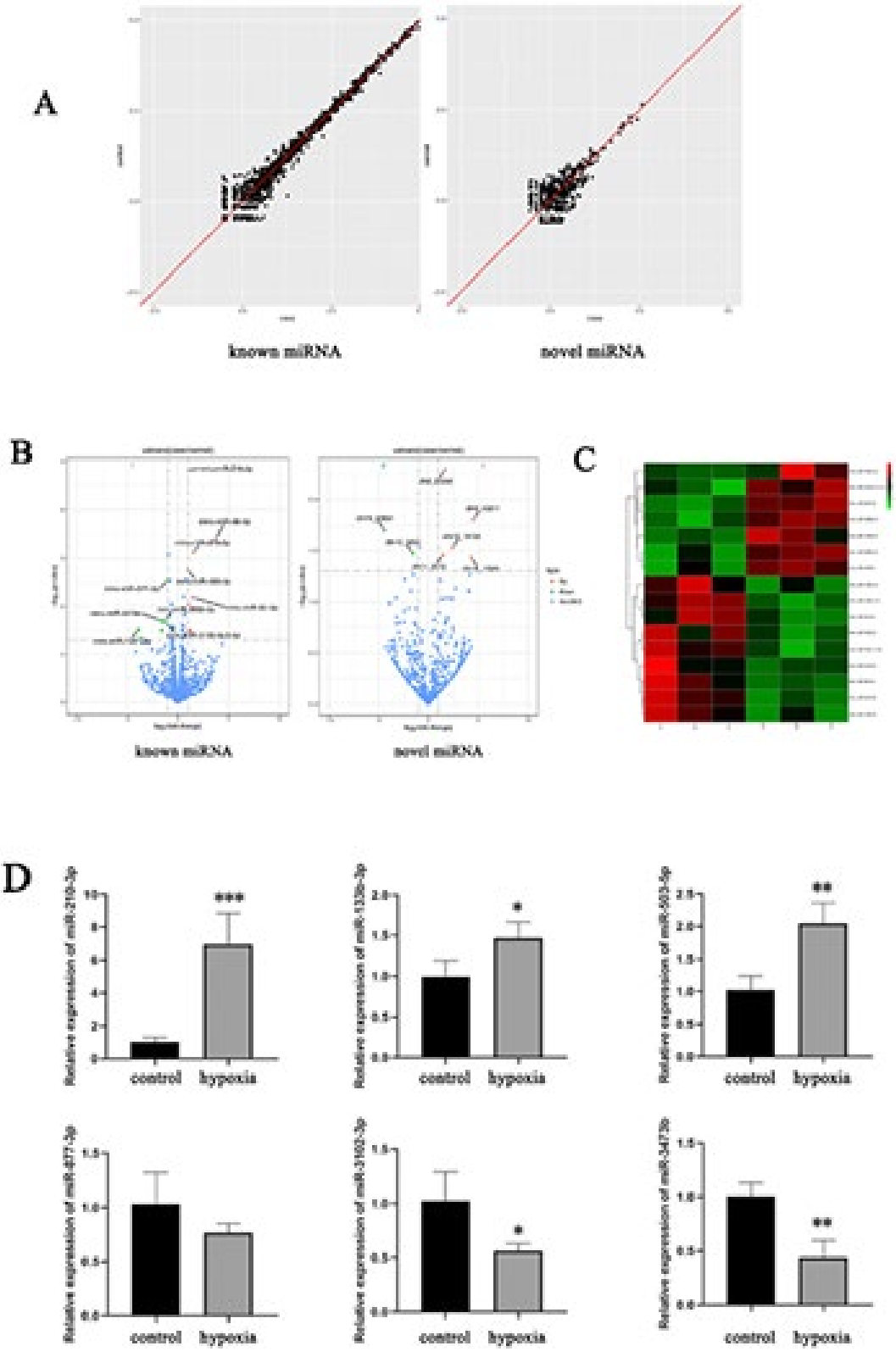

Figure 2. (A) Scatter plot illustrating differentially expressed miRNAs. (B) Scatter plot of differentially expressed miRNAs between the control and hypoxia groups. The *x*-axis illustrates the logarithmic value of the fold change in gene expression levels, and the *y*-axis represents the negative logarithmic value of the *p* value of the change in gene expression. Genes with significant differences are denoted by red and green dots. (C) Heatmap showing cluster analysis for known differentially expressed miRNAs. Each column in the heatmap indicates a specific sample, and each row represents a different gene. Red indicates high expression and green indicates low expression. (D) Relative expression levels of six miRNAs that were differentially expressed between samples from the normal control and hypoxia treatment groups as determined by qRT-PCR. *$p < .05$, **$p < .01$ and ***$p < .001$.

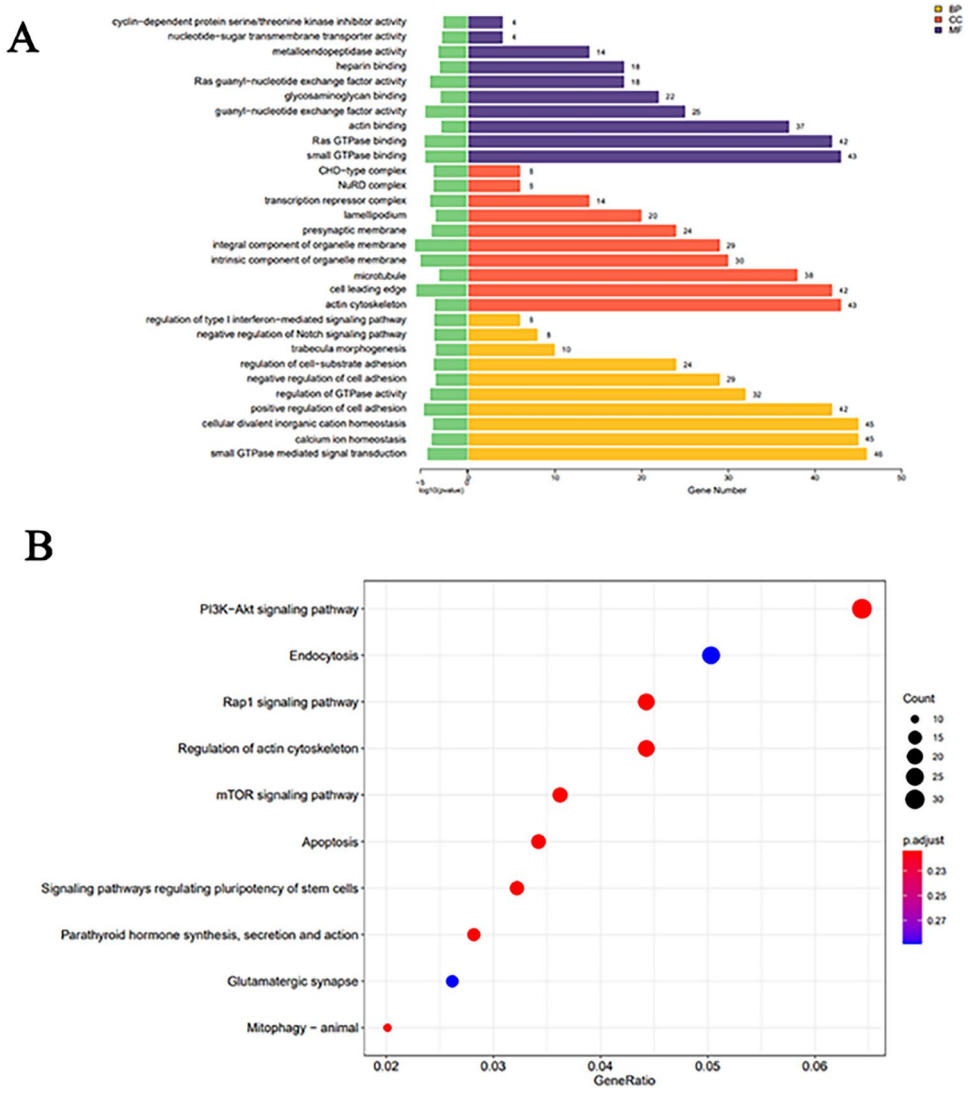

Figure 3. (A) Bar chart displaying GO enrichment analysis results for differentially expressed miRNAs. (B) Scatter plot representing KEGG enrichment analysis results for differentially expressed miRNAs.

miRNAs: mmu-miR-877-3p, mmu-miR-3473b, mmu-miR-3102-5p.2-5p) and validated their upregulation and downregulation by RT-qPCR. Results of RT-qPCR were consistent with those of the RNA-seq data (Figure 2(D)).

3.3. Differential miRNA target gene enrichment analysis

Using miRanda and RNA hybrids, we forecasted the target genes for the differentially expressed miRNAs and identified the intersections of the two sets of predictions as the final result. GO analysis was performed to annotate and analyse the target genes, which were found to be enriched in 'microtubule', 'small GTPase mediated signal transduction', 'actin cytoskeleton' and 'small GTPase binding' (Figure 3(A)). KEGG analysis revealed that target genes of the differentially expressed miRNAs were enriched in 'mTOR signalling pathway', 'endocytosis', 'PI3K-Akt signalling pathway', 'regulation of actin cytoskeleton', 'Signaling pathways regulating pluripotency of stem cells' and 'apoptosis' (Figure 3(B)).

3.4. Lentivirus transfection

Based on sequencing results, we initially transfected CPCs with the most representative miRNA-210-3p inhibitor and subjected them to hypoxic conditions. The expression level of miRNAs in each group was quantified using RT-qPCR (Figure 4(A)). In addition, ARY015 was used to assess the expression of 53 angiogenesis-related proteins in each group's conditioned medium and cell protein lysates.

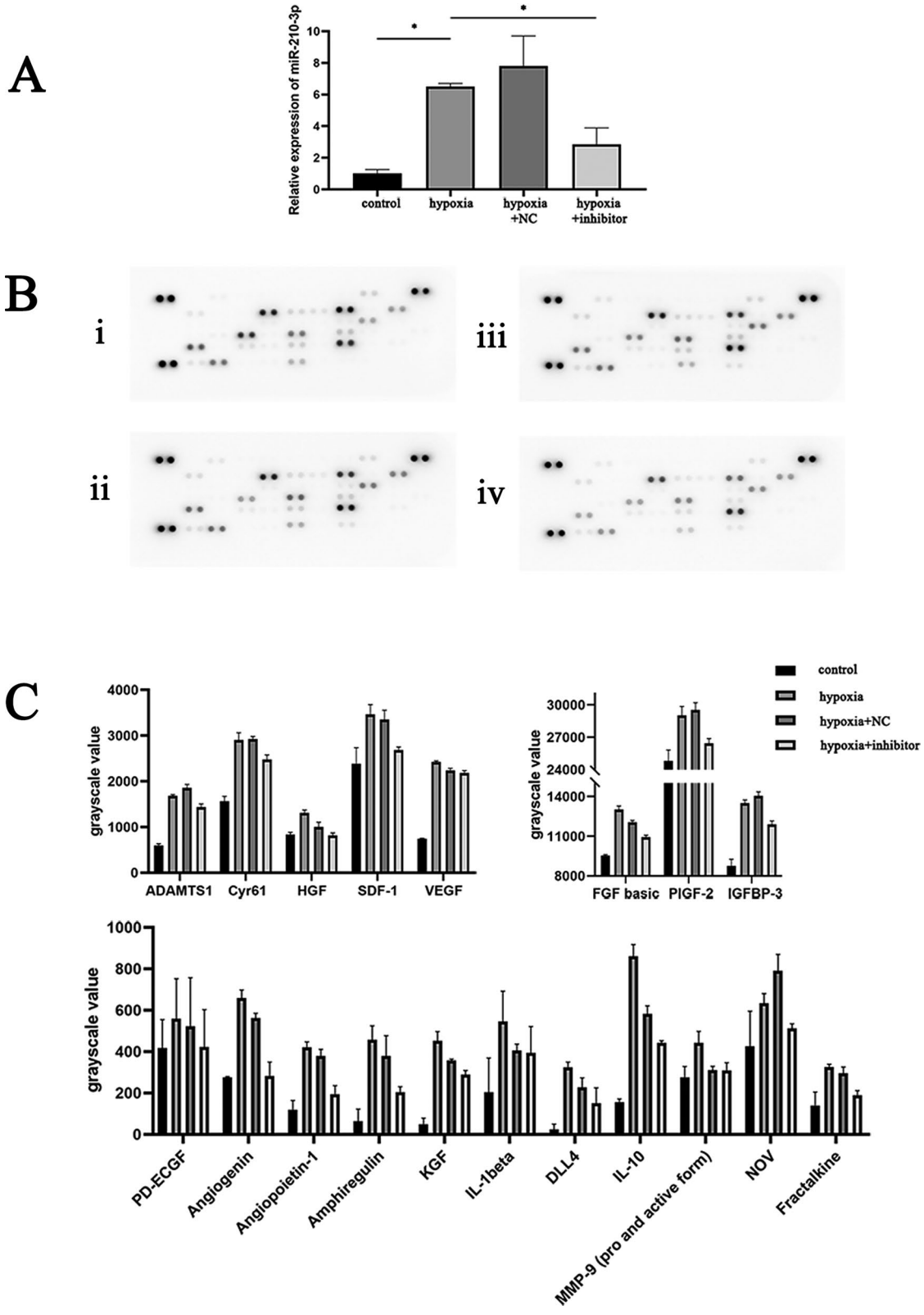

Figure 4. (A) qRT-PCR analysis of CPCs transfected with miR-210-3p inhibitor. *$p < .05$. (B) Protein chip image of the cell culture supernatant in the indicated groups. (i) Control group, (ii) hypoxia group, (iii) NC + hypoxia group and (iv) miR-210-3p inhibitor transfection + hypoxia group. (C) Bar graph analysis of protein chip results for cell culture supernatant from the indicated groups.

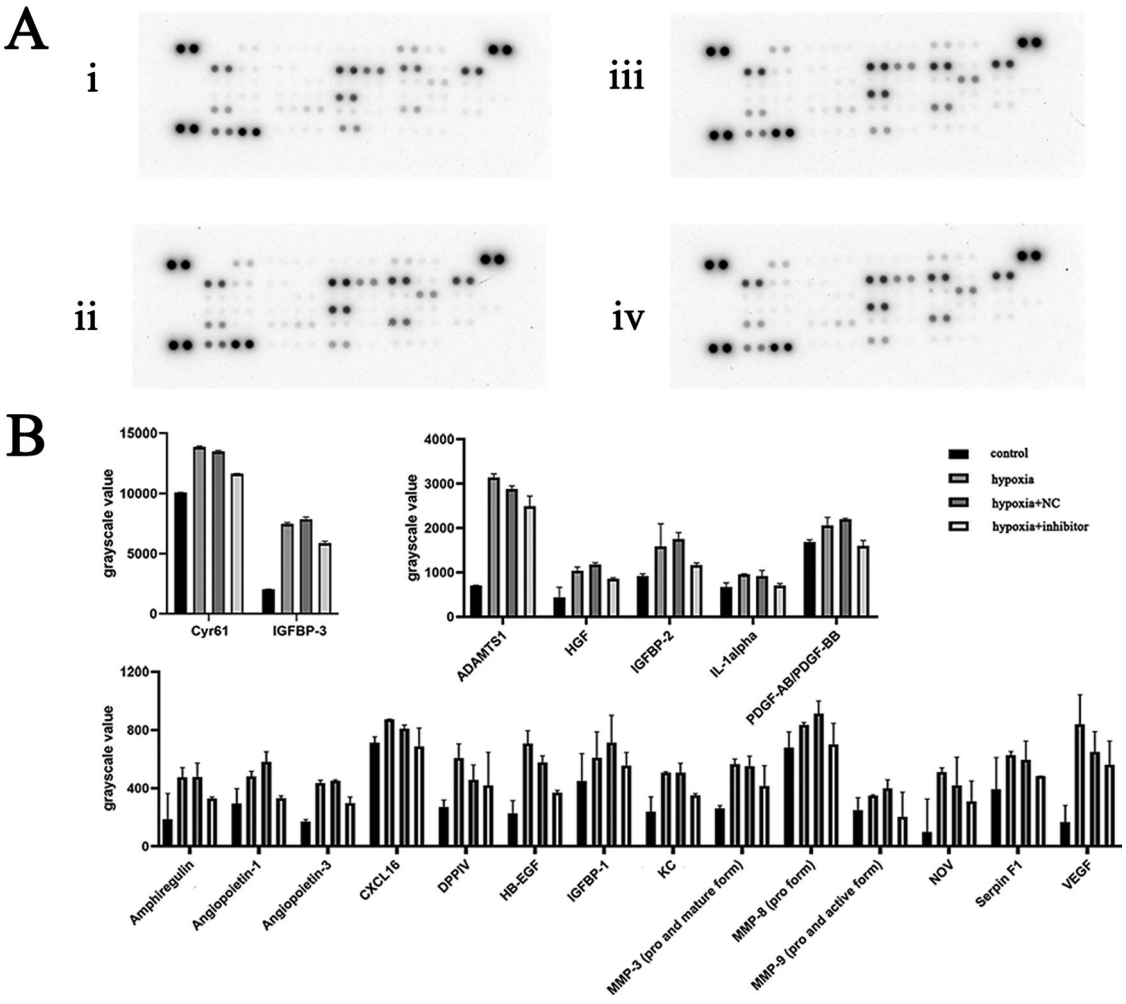

Figure 5. (A) Protein chip results image of cell lysate for the indicated groups. (i) Control group, (ii) hypoxia group, (iii) NC + hypoxia group and (iv) miR-210-3p inhibitor transfection + hypoxia group. (B) Bar graph analysis of protein chip results for cell lysate for the indicated groups.

3.5. Changes in angiogenesis-related proteins

Expression of 53 angiogenesis-related cytokines in cell culture supernatants and cell lysates of CPCs samples from four groups: control group, hypoxia group, miR-210-3p inhibitor transfection + hypoxia group and NC + hypoxia group were determined using the protein chip technology (Figures 4(B,C) and 5). Background correction was performed, and protein chip results showed that CPCs could express and secrete cytokines such as angiopoietin-1, amphiregulin, FGF basic, CXCL16, Cyr61, HGF, fractalkine, PlGF-2, SDF-1 and VEGF, which involved in angiogenesis. Protein expressions of Cyr61, HGF, VEGF, angiogenin and angiopoietin-1 in cell lysates of the hypoxia group were significantly higher compared to the control group ($p < .05$). Protein expressions of FGF basic, angiogenin, angiopoietin-1, Cyr61 and IGFBP-3 in cell protein lysates of the miR-210-3p inhibitor transfection + hypoxia group were significantly suppressed, compared to the hypoxia group ($p < .05$). Protein levels of Cyr61, fractalkine, VEGF and angiogenin in hypoxia group cell culture supernatants were significantly greater than in the control group ($p < .05$). The protein expression of PDGF-AB, angiogenin, CXL16, Cyr61 and IL-1alpha between the miR-210-3p inhibitor transfection + hypoxia group and hypoxia group was significantly different ($p < .05$).

3.6. Paracrine effects of CPCs on angiogenesis of endothelial cells

To assess the effects of CPCs on endothelial cells, a series of *in vitro* functional tests were performed by treating CMECs with CM from different groups. The CCK-8 proliferation assay revealed that CMECs treated with CM-H exhibited significantly increased proliferation levels, compared with the CM-C group. Proliferation of the CMECs treated with CM-miR was significantly inhibited, compared to the CM-H group (Figure 6(A)). The

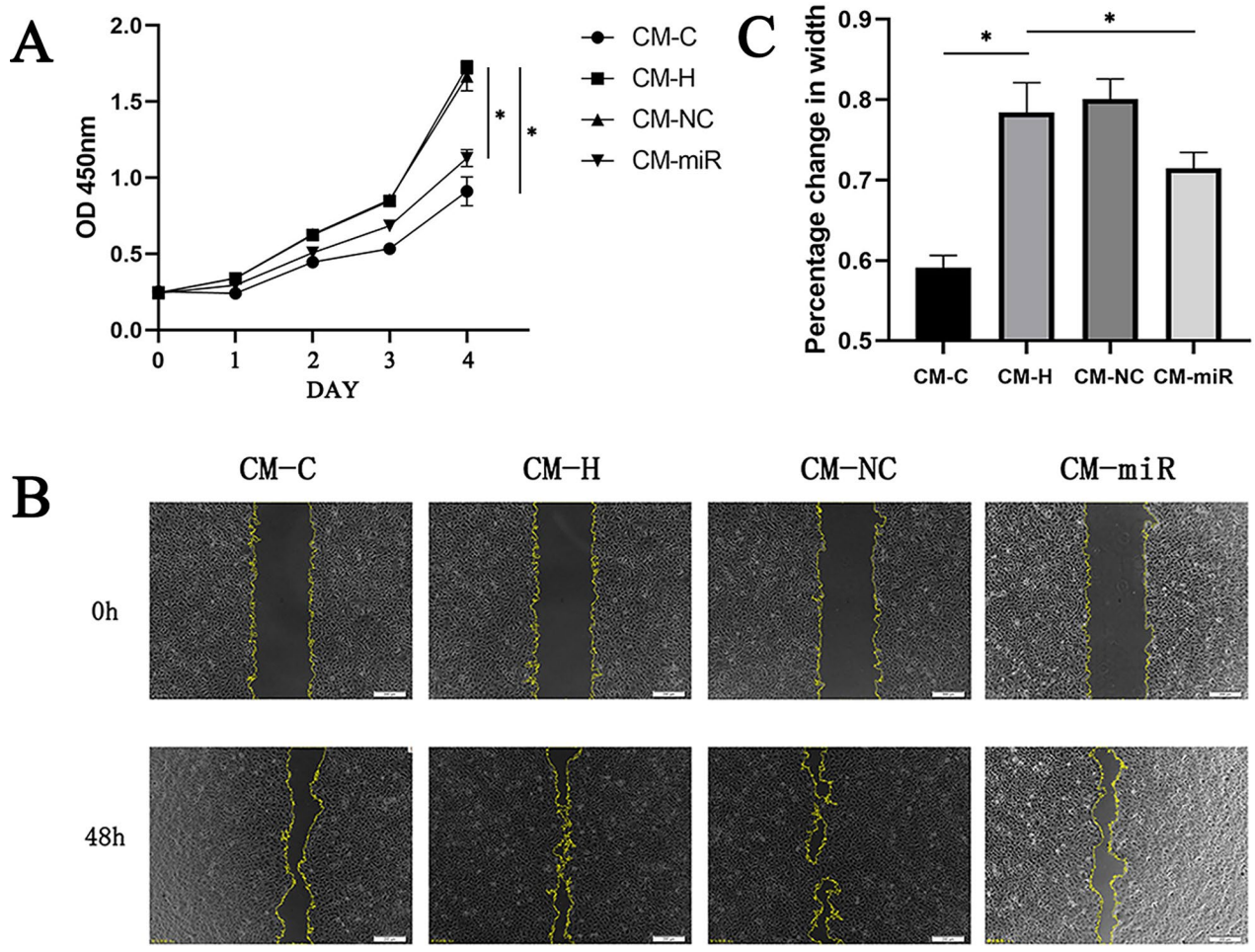

Figure 6. (A) The effect of four different culture media on CMEC proliferation. *$p < .05$. (B) Detection of the effect of four different cell culture media on CMEC migration ability as determined by the scratch assay. (C) Statistical analysis of the results from experiment B. *$p < .05$.

conditioned medium of CPCs after hypoxia promoted endothelial cell proliferation, while the conditioned medium of CPCs transfected with the miR-210-3p inhibitor after hypoxia inhibited endothelial cell proliferation.

Scratch wound healing assays were performed to measure the effects of CPCs on CMEC migration. Compared with the CM-C group, when CMECs were incubated with CM-H, there was a significant increase in endothelial cell migration, as determined by the migration region (Figure 6(B)). The Transwell assay, another commonly used method for measuring cell migration, was used to confirm the pro-migratory potential of CPCs (Figure 7(A)). The CM-H group treated CMECs exhibited significant migrations compared to the CM-C group. However, compared with the CM-H group, the CM-miR group significantly inhibited CMECs migration distance and membrane penetration (Figures 6(C) and 7(C)). Consequently, the conditioned medium derived from hypoxia treated CPCs exhibited a notable enhancement in the migratory potential of endothelial cells. In contrast, the conditioned medium obtained from hypoxia-treated CPCs transfected with the miR-210-3p inhibitor exerted a suppressive effect on endothelial cell migration.

An *in vitro* angiogenesis assay was also performed to assess the influence of miR-210-3p inhibitors on tube formation abilities of hypoxia-treated CPCs in CMECs (Figure 7(B)). Compared with the CM-C group, the CM-H group exhibited a significant increase in tubular lengths of CMECs and enhanced endothelial cell tube formation abilities. However, under the same conditions, the length of endothelial cell tubules cultured in CM-miR decreased (Figure 7(D)). Thus, the conditioned medium of CPCs after hypoxia enhanced endothelial cell tube formation abilities, whereas the conditioned medium of CPCs transfected with the miR-210-3p inhibitor after hypoxia inhibited endothelial cell tube formation.

In conclusion, miR-210-3p may be involved in paracrine functions of CPCs.

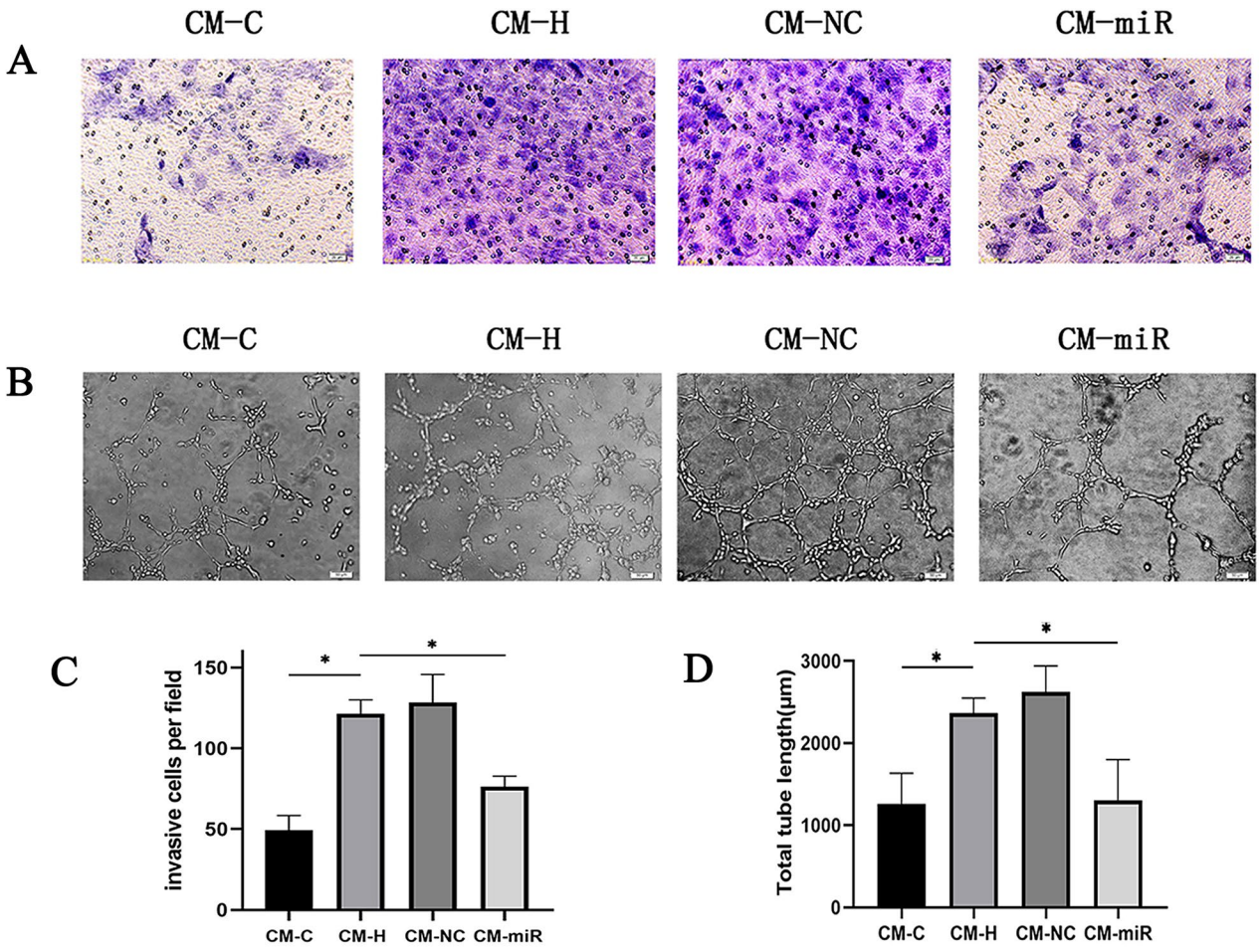

Figure 7. (A) Analysis of changes in the migration ability of CMECs across four distinct cell culture conditions using the Transwell migration assay. (B) Analysis of changes in the tube formation ability of CMECs across four distinct cell culture conditions using the tube formation assay. (C) Statistical examination of experiment A outcomes. *$p < .05$. (D) Statistical examination of experiment B outcomes. *$p < .05$.

4. Discussion

Given that they do not differentiate into mature cardiomyocytes myocytes even after a year, CPCs are known to produce long-lasting functional improvements [22]. For instance, they were reported to enhance left ventricular function by releasing mediators that regulate the contractile characteristics of the host heart [23]. Moreover, it should be noted that the therapeutic potential of CPCs in preclinical models of ICM, including acute and age-related myocardial infarction, has been thoroughly investigated. The positive benefits of CPC administration in these models have been documented in at least 26 studies from independent laboratories worldwide [24]. CPC treatment has been demonstrated to enhance heart function after acute, subacute or age-related myocardial infarction, frequently in conjunction with a smaller scar [24]. These findings collectively provide robust preclinical evidence for the therapeutic potential of CPCs.

We isolated CPCs and subjected them to hypoxic treatment to mimic ischemic heart disease. Sequencing of both the normal control and hypoxia-treated CPCs was performed to identify the differentially expressed miRNAs. Among them, miR-210-3p was significantly elevated in hypoxia-treated CPCs. MiR-210-3p expressions have been reported to be increased in the myocardium of patients with acute myocardial infarction [25] and in animal models of myocardial ischemia [26]. MiR-210, the most consistently and robustly induced miRNA under hypoxia [27], is involved in regulation of mitochondrial functions, apoptosis and cell proliferation [28]. In addition, miR-210 can regulate endothelial cell functions and promote angiogenesis under hypoxic conditions, thereby improving cardiac functional recovery after ischemic injury [29]. These findings indicate that miR-210-3p may have therapeutic implications in ischemic diseases and cancer. Our discovery of miR-210-3p overexpression in hypoxia-treated CPCs underlines the possible significance of

this miRNA in controlling the functions of CPCs under hypoxic settings. In the context of recent or old myocardial infarction, there is a considerable consensus at the preclinical stage regarding the potential benefits of cardiac CPCs. The available data strongly confirm the therapeutic effects of CPCs in preclinical heart failure treatment [30]. Moreover, considering the influence of miR-210-3p on the paracrine functions and angiogenesis of CPCs, these findings underscore the promising therapeutic implications of miR-210-3p in the context of ischemic heart disease.

We investigated the effects of miR-210-3p on expressions of angiogenic factors in CPCs under hypoxic conditions. To achieve this, we divided our experiment into four groups: control group, hypoxia group, miR-210-3p inhibitor-transfected and hypoxia group and NC transfected and hypoxia group. The supernatants and intracellular proteins were obtained from the four groups of CPC samples and used to measure the expressions of various angiogenic factors using ARY015. Protein chip analysis revealed that CPCs could secrete multiple endothelial cell-related proteins, including MCP-1, IL-1α, endothelin-1 and Cyr61. Moderate levels of endothelin-1 can stimulate VEGF secretion and promote endothelial cell migration, whereas excess secretion can result in vasoconstriction and promote atherosclerosis [31]. Cyr61 is highly expressed throughout development and plays a crucial role in promoting cardiovascular development and maintaining vascular integrity [32,33]. Endothelial cells also express MCP-1 and IL-1α. Analysis of protein chip results showed that CPCs have some endothelial cell functions, implying that CPCs originate from endothelial cells. Moreover, CPCs express various pro-angiogenic factors, including IL-1β, FGF basic, Cyr61, PlGF-2, GM-CSF and endothelin-1. FGF basic is a potent angiogenic factor that promotes angiogenesis, particularly in myocardial ischemia and hypoxia, by breaking down the capillary basement membrane and encouraging endothelial cell proliferation as well as migration [34]. The PlGF-2 can increase endothelial cell proliferation and migration while also promoting angiogenesis [35]. Endothelial cells secrete GM-CSF, which affects them through autocrine actions. GM-CSF is involved in angiogenesis by promoting early endothelial tube formation and late-stage neovascularization maturation, which helps to restore cardiac functions and increase angiogenesis [36,37]. Hypoxia treatment better mimics the state of cells in the body and is one of the ways for enhancing the biological functions of CPCs. After hypoxia treatment, Cyr61, FGF basic, HGF, IL-1β, PD-ECGF, SDF-1 and VEGF were significantly increased, indicating that hypoxia enhanced the secretion functions of CPCs. RajendranNair et al. concluded that CPCs can promote angiogenesis under hypoxic conditions [38]. Silencing miR-210-3p in CPCs after hypoxia treatment suppressed the secretion of proteins that promote angiogenesis, including Cyr61, FGF basic, HGF, IL-1β and PlGF-2. Protein chip analysis of supernatants and intracellular proteins of CPCs revealed slight differences, which may be due to different mechanisms by which miR-210-3p regulated angiogenesis. However, the overall direction of the results was consistent. In summary, under hypoxic conditions, miR-210-3p plays a crucial role in regulating the secretion of angiogenic factors by CPCs.

We investigated the paracrine effects and angiogenic potential of CPCs under different conditions. We co-cultured CMEMs with four different types of CPCs-conditioned medium and discovered that CM-H significantly improved endothelial cell proliferation, migration and tube formation, whereas CM-miR suppressed these effects. These findings imply that CPCs may exhibit pro-angiogenic effects via paracrine pathways mediated by miR-210-3p. The paracrine effects of CPCs are important in angiogenesis and tissue repair [39]. Our findings are consistent with these studies and suggest that upregulation of miR-210-3p in hypoxia-treated CPCs enhances their paracrine functions by regulating the secretion of pro-angiogenic factors such as VEGF, angiopoietin-1 and FGF basic, to promote angiogenesis in ischemic heart disease. Inhibition of endothelial cell proliferation, migration and tube formation by CM-miR further supports the potential therapeutic applications of miR-210-3p in ischemic heart disease. However, the specific factors involved in this process and their underlying molecular mechanisms are not fully understood.

This study is among the first to investigate the roles of miR-210-3p in regulating the paracrine functions of CPCs and its effects on angiogenesis. We found that miR-210-3p plays a critical role in mediating the effects of hypoxia on CPCs and their paracrine functions. However, this study has some limitations. Expressions of angiogenic factors in CPCs under diverse settings were not investigated, which further supports the impact of miR-210-3p on their paracrine functions. Moreover, the mechanisms underlying the miR-210-3p-mediated regulation of target genes should be investigated further. Finally, the study only utilized in vitro cell culture models. Validations of experimental results in vivo should be performed to ensure the feasibility and accuracy of the findings. The results of this study suggest that miR-210-3p is a viable therapeutic target for ischemic

heart disease. Additionally, exploring the roles of miR-210-3p in other cardiovascular diseases may shed light on its broad implications for cardiovascular health. Finally, studies should be performed to uncover the complex network relationship between miRNAs, CPCs and cardiovascular diseases, which could pave the way for novel treatment strategies and preventive measures.

5. Conclusions

This is one of the first studies to investigate the roles of miR-210-3p in regulating the paracrine functions of CPCs and its impact on angiogenesis. Our findings elucidate on the functions of CPCs and the involvement of miR-210-3p in angiogenesis, which are potential therapeutic targets.

Author contributions

All the authors contributed to the conception and design of the study. Material preparation, data collection and analysis were performed by LS, GF, GY, ZY and CG. The first draft of the manuscript was written by Louyi Shen, and all the authors commented on the previous versions of the manuscript. All the authors have read and approved the final manuscript.

Ethics statement

The animal study was reviewed and approved by the Nanning Medical University Ethics Committee.

Disclosure statement

The authors declare that the research was conducted in the absence of any commercial or financial relationships that could be construed as potential conflicts of interest.

Funding

This work was supported by the Guangxi Natural Science Foundation (Grant No. 2020GXNSFDA297014) and the Innovative Research Team Project of the Guangxi Natural Science Foundation (Grant No. 2018GXNSFGA281006).

ORCID

Chun Gui http://orcid.org/0000-0002-4484-3339

Data availability statement

The raw data supporting the conclusions of this article will be made available by the authors without undue reservation.

References

[1] Katikireddy CK, Acharya T. Myocardial segmental thickness variability on echocardiography is a highly sensitive and specific marker to distinguish ischemic and non-ischemic dilated cardiomyopathy in new onset heart failure. Int J Cardiovasc Imaging. 2019;35(5):1–15. doi: 10.1007/s10554-018-01515-3.

[2] Tang XL, Rokosh G, Sanganalmath SK, et al. Intracoronary administration of cardiac progenitor cells alleviates left ventricular dysfunction in rats with a 30-day-old infarction. Circulation. 2010;121(2):293–305. doi: 10.1161/CIRCULATIONAHA.109.871905.

[3] Beltrami AP, Barlucchi L, Torella D, et al. Adult cardiac stem cells are multipotent and support myocardial regeneration. Cell. 2003;114(6):763–776. doi: 10.1016/s0092-8674(03)00687-1.

[4] Li Q, Guo Y, Ou Q, et al. Intracoronary administration of cardiac stem cells in mice: a new, improved technique for cell therapy in murine models. Basic Res Cardiol. 2011;106(5):849–864. doi: 10.1007/s00395-011-0180-1.

[5] Hong KU, Guo Y, Li QH, et al. c-kit+cardiac stem cells alleviate post-myocardial infarction left ventricular dysfunction despite poor engraftment and negligible retention in the recipient heart. PLOS One. 2014;9(5):e96725. doi: 10.1371/journal.pone.0096725.

[6] Tiwari A, Mukherjee B, Dixit M. MicroRNA key to angiogenesis regulation: miRNA biology and therapy. Curr Cancer Drug Targets. 2018;18(3):266–277. doi: 10.2174/1568009617666170630142725.

[7] Wang Y, Lee CG. MicroRNA and cancer – focus on apoptosis. J Cell Mol Med. 2009;13(1):12–23. doi: 10.1111/j.1582-4934.2008.00510.x.

[8] Harris TA, Yamakuchi M, Ferlito M, et al. MicroRNA-126 regulates endothelial expression of vascular cell adhesion molecule 1. Proc Natl Acad Sci USA. 2008;105(5):1516–1521. doi: 10.1073/pnas.0707493105.

[9] Wang J, Huang W, Xu R, et al. MicroRNA-24 regulates cardiac fibrosis after myocardial infarction. J Cell Mol Med. 2012;16(9):2150–2160. doi: 10.1111/j.1582-4934.2012.01523.x.

[10] Van Rooij E, Sutherland LB, Thatcher JE, et al. Dysregulation of microRNAs after myocardial infarction reveals a role of miR-29 in cardiac fibrosis. Proc Natl Acad Sci USA. 2008;105(35):13027–13032. doi: 10.1073/pnas.0805038105.

[11] De Gonzalo-Calvo D, Iglesias-Gutiérrez E, Llorente-Cortés V. Epigenetic biomarkers and cardiovascular disease: circulating microRNAs. Rev Esp Cardiol. 2017;70(9):763–769. doi: 10.1016/j.recesp.2017.02.027.

[12] Kalayinia S, Arjmand F, Maleki M, et al. MicroRNAs: roles in cardiovascular development and disease. Cardiovasc Pathol. 2021;50:107296. doi: 10.1016/j.carpath.2020.107296.

[13] Hu S, Huang M, Li Z, et al. MicroRNA-210 as a novel therapy for treatment of ischemic heart disease. Circulation. 2010;122(11 Suppl.):S124–S131. doi: 10.1161/CIRCULATIONAHA.109.928424.

[14] Sirish P, López JE, Li N, et al. MicroRNA profiling predicts a variance in the proliferative potential of cardiac progenitor cells derived from neonatal and adult murine hearts. J Mol Cell Cardiol. 2012;52(1):264–272. doi: 10.1016/j.yjmcc.2011.10.012.

[15] Wang J, Greene SB, Bonilla-Claudio M, et al. *Bmp*-signaling regulates myocardial differentiation from cardiac progenitors through a microRNA-mediated mechanism. Dev Cell. 2010;19(6):903–912. doi: 10.1016/j.devcel.2010.10.022.

[16] Anand S, Majeti BK, Acevedo LM, et al. MicroRNA-132-mediated loss of p120RasGAP activates the endothelium to facilitate pathological angiogenesis. Nat Med. 2010;16(8):909–914. doi: 10.1038/nm.2186.

[17] Anand S. A brief primer on microRNAs and their roles in angiogenesis. Vasc Cell. 2013;5(1):2. doi: 10.1186/2045-824X-5-2.

[18] Spengler RM, Oakley CK, Davidson BL. Functional microRNAs and target sites are created by lineage-specific transposition. Hum Mol Genet. 2014;23(7):1783–1793. doi: 10.1093/hmg/ddt569.

[19] Crouser ED, Hamzeh NY, Maier LA, et al. Exosomal microRNA for detection of cardiac sarcoidosis. Am J Respir Crit Care Med. 2017;196(7):931–934. doi: 10.1164/rccm.201611-2183LE.

[20] Xiao K, Thum T. Exosomal microRNAs released by pediatric cardiac progenitor cells. Circ Res. 2017;120(4):607–609. doi: 10.1161/CIRCRESAHA.117.310443.

[21] Livak KJ, Schmittgen TD. Analysis of relative gene expression data using real-time quantitative PCR and the 2(–Delta Delta C(T)) method. Methods. 2001;25(4):402–408. doi: 10.1006/meth.2001.1262.

[22] Tang XL, Li Q, Rokosh G, et al. Long-term outcome of administration of c-kit(POS) cardiac progenitor cells after acute myocardial infarction: transplanted cells do not become cardiomyocytes, but structural and functional improvement and proliferation of endogenous cells persist for at least one year. Circ Res. 2016;118(7):1091–1105. doi: 10.1161/CIRCRESAHA.115.307647.

[23] Bolli R, Tang XL, Sanganalmath SK, et al. Intracoronary delivery of autologous cardiac stem cells improves cardiac function in a porcine model of chronic ischemic cardiomyopathy. Circulation. 2013;128(2):122–131. doi: 10.1161/CIRCULATIONAHA.112.001075.

[24] Bolli R, Tang XL, Guo Y, et al. After the storm: an objective appraisal of the efficacy of c-kit+cardiac progenitor cells in preclinical models of heart disease. Can J Physiol Pharmacol. 2021;99(2):129–139. doi: 10.1139/cjpp-2020-0406.

[25] Wang Y, Pan X, Fan Y, et al. Dysregulated expression of microRNAs and mRNAs in myocardial infarction. Am J Transl Res. 2015;7(11):2291–2304.

[26] Diao H, Liu B, Shi Y, et al. MicroRNA-210 alleviates oxidative stress-associated cardiomyocyte apoptosis by regulating BNIP3. Biosci Biotechnol Biochem. 2017;81(9):1712–1720. doi: 10.1080/09168451.2017.1343118.

[27] Kulshreshtha R, Ferracin M, Wojcik SE, et al. A microRNA signature of hypoxia. Mol Cell Biol. 2007;27(5):1859–1867. doi: 10.1128/MCB.01395-06.

[28] Chan SY, Zhang YY, Hemann C, et al. MicroRNA-210 controls mitochondrial metabolism during hypoxia by repressing the iron–sulfur cluster assembly proteins ISCU1/2. Cell Metab. 2009;10(4):273–284. doi: 10.1016/j.cmet.2009.08.015.

[29] Huang X, Le QT, Giaccia AJ. MiR-210 – micromanager of the hypoxia pathway. Trends Mol Med. 2010;16(5):230–237. doi: 10.1016/j.molmed.2010.03.004.

[30] Bolli R, Hare JM, March KL, et al. Rationale and design of the CONCERT-HF trial (combination of mesenchymal and c-kit(+) cardiac stem cells as regenerative therapy for heart failure). Circ Res. 2018;122(12):1703–1715. doi: 10.1161/CIRCRESAHA.118.312978.

[31] Dawas K, Loizidou M, Shankar A, et al. Angiogenesis in cancer: the role of endothelin-1. Ann R Coll Surg Engl. 1999;81(5):306–310.

[32] Mo FE, Muntean AG, Chen CC, et al. CYR61 (CCN1) is essential for placental development and vascular integrity. Mol Cell Biol. 2002;22(24):8709–8720. doi: 10.1128/MCB.22.24.8709-8720.2002.

[33] Jun JI, Lau LF. The matricellular protein CCN1 induces fibroblast senescence and restricts fibrosis in cutaneous wound healing. Nat Cell Biol. 2010;12(7):676–685. doi: 10.1038/ncb2070.

[34] Amann K, Faulhaber J, Campean V, et al. Impaired myocardial capillarogenesis and increased adaptive capillary growth in FGF2-deficient mice. Lab Invest. 2006;86(1):45–53. doi: 10.1038/labinvest.3700359.

[35] Wu M, Claus P, Vanden Driessche N, et al. Placental growth factor 2 – a potential therapeutic strategy for chronic myocardial ischemia. Int J Cardiol. 2016;203:534–542. doi: 10.1016/j.ijcard.2015.10.177.

[36] Fang Y, Shen J, Yao M, et al. Granulocyte-macrophage colony-stimulating factor enhances wound healing in diabetes via upregulation of proinflammatory cytokines. Br J Dermatol. 2010;162(3):478–486. doi: 10.1111/j.1365-2133.2009.09528.x.

[37] Mann A, Niekisch K, Schirmacher P, et al. Granulocyte-macrophage colony-stimulating factor is essential for normal wound healing. J Investig Dermatol Symp Proc. 2006;11(1):87–92. doi: 10.1038/sj.jidsymp.5650013.

[38] RajendranNair DS, Karunakaran J, Nair RR. Sub-physiological oxygen levels optimal for growth and survival of human atrial cardiac stem cells. Mol Cell Biochem. 2017;432(1–2):109–122. doi: 10.1007/s11010-017-3002-4.

[39] Bao L, Meng Q, Li Y, et al. C-kit positive cardiac stem cells and bone marrow-derived mesenchymal stem cells synergistically enhance angiogenesis and improve cardiac function after myocardial infarction in a paracrine manner. J Card Fail. 2017;23(5):403–415. doi: 10.1016/j.cardfail.2017.03.002.